Geometry and Origin of Fault-Related Folds in Extensional Settings[1]

Roy W. Schlische[2]

ABSTRACT

The majority of folds in extensional tectonic settings are associated with normal fault systems over a wide range of scales. The hinges of longitudinal folds are subparallel to associated faults, whereas those of transverse folds are oriented at a high angle to the related normal faults. Longitudinal folds include drag folds (hanging-wall synclines and footwall anticlines), reverse-drag folds (hanging-wall anticlines and footwall synclines), and rollover folds (hanging-wall anticlines). Drag folds form as a result of fault propagation into monoclinal warps present at the fault tips; some may form as a result of frictional drag and differential compaction. Reverse-drag folds develop because displacement decreases with distance from the fault surface. Rollover folds are produced by movement along gravity-driven listric faults in thick sedimentary successions. Drag folds have a smaller wavelength than reverse-drag or rollover folds and may be superimposed on these larger structures. Basin-scale synclines are the largest type of transverse folds and are manifested in plan view by basin outlines that are concave toward the border fault. These folds form because displacement is greatest near the center of the map trace of the border fault and decreases toward its along-strike ends; this is a scale-invariant feature of most normal faults. Transverse folds are also associated with segmented fault systems: hanging-wall synclines are located near the centers of fault segments, whereas hanging-wall anticlines are found at segment boundaries where the fault segments commonly overlap. Some transverse folds may be caused by movement along an undulatory fault surface. Many folds in extensional tectonic settings form syndepositionally and control stratal thickness and facies relationships.

INTRODUCTION

Folds have long been recognized as important structural traps. Most folds are associated with contractional tectonic environments, transpressional regimes, and salt diapirism. However, many types of folds and flexures are also present in extensional tectonic settings. Fault-parallel folds, such as drag folds and rollover folds (e.g., Hamblin, 1965; Harding, 1984), have received the most attention in the literature, and form as a result of movement on the associated normal fault systems. Fault-perpendicular folds have been recognized since the work of Wheeler (1939) but have received considerably less attention. These folds also form in response to displacement on normal fault systems (e.g., Withjack and Drickman Pollock, 1984; Schlische, 1993) and, as shown in this paper, are as common and important as fault-parallel folds.

This paper reviews the types, geometry, and mechanisms of formation of folds and flexures in extensional settings; it also reviews the features of normal fault systems relevant to folding. The geometries of the various types of folds are illustrated with examples from the Basin and Range, Mesozoic rift system of eastern North America, the North Sea, and the Gulf of Suez. Emphasis is placed on fault-perpendicular folds. The significance of these folds to hydrocarbon exploration is also briefly addressed.

FEATURES OF NORMAL FAULTS

Recent research on normal fault systems has documented that displacement is commonly greatest at or near the center of the fault and decreases to zero at the fault tips (Figure 1a; Chapman et al., 1978; Muraoka and Kamata, 1983; Barnett et al., 1987;

[1]Manuscript received December 27, 1994; revised manuscript received May 10, 1995; final acceptance June 30, 1995.

[2]Department of Geological Sciences, Rutgers University, Busch Campus, Piscataway, New Jersey 08855-1179.

Research was supported by the National Science Foundation (EAR-9017785), a Henry Rutgers Research Fellowship, and Grants-in-Aid-of-Research from Sigma Xi and the Geological Society of America. My views of fold geometries in extensional settings benefited from discussions with Mark Anders, Paul Olsen, Dave Reynolds, Alan Roberts, and Martha Withjack. I thank Dave Reynolds for sharing unpublished data with me. Rolf Ackermann, Albert Bally, James Lowell, and John Shelton critically reviewed the manuscript.

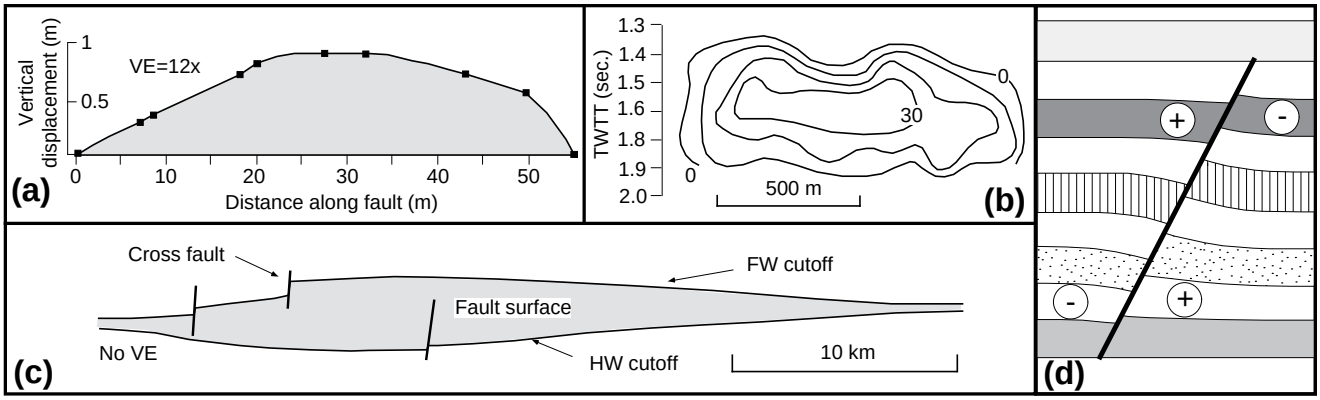

Figure 1—Displacement geometry associated with normal faults. (a) Vertical displacement derived from variation in scarp height on a normal fault within the Volcanic Tableland, California. Modified from Dawers et al. (1993). (b) Contours of equal fault displacement in milliseconds for normal fault imaged on a grid of closely spaced seismic reflection profiles from the North Sea. Modified from Barnett et al. (1987). TWTT = two-way traveltime. (c) Horizon-separation diagram for the Tiim Phonolite on the Saimo fault in the Kenya rift valley. Modified from Chapman et al. (1978). FW = footwall; HW = hanging wall. (d) Reverse-drag folds produced by decrease in displacement with distance from a blind normal fault. Deformation quadrants are dilational (+) and contractional (–). Modified from Barnett et al. (1987).

Walsh and Watterson, 1987; Dawers et al., 1993; Young et al., 1995). For isolated normal faults that do not intersect the Earth's surface (blind faults), the zero-displacement contour (tip-line loop) of the fault plane has an elliptical geometry (Figure 1b), with the short axis of the ellipse parallel to the slip direction. For large normal faults, the elliptical fault surface geometry may be truncated by the Earth's surface and/or the base of the seismogenic crust.

The displacement field described in the previous paragraph is a scale-invariant feature of normal faults. For the faults illustrated in Figure 1a–c, the lengths of the faults vary from a few tens of meters to tens of kilometers. Similar displacement geometries have been observed on micro-normal faults with lengths in the range of 0.5 cm to 100 cm (Young et al., 1995). Because of this displacement geometry, faulted layers in the hanging wall are expected to exhibit a synclinal geometry, and those in the footwall exhibit an anticlinal geometry (Figure 1c). Given the scale independence of fault-displacement geometry, associated folds should be similarly scale independent.

For large (kilometer-scale) faults, the synclinal depression defines an elongate sedimentary basin. The uplifted footwall may be an important source of sediment for the basin. The relative amounts of footwall uplift and hanging-wall subsidence are variable; ratios of 1:1, 1:2, and 1:5 have been reported in the literature (Stein and Barrientos, 1985; Barrientos et al., 1987; Stein et al., 1988). For isolated blind normal faults, the amounts of hanging-wall subsidence and footwall uplift are approximately equal (Gibson et al., 1989). For faults that intersect the Earth's surface, the relative amount of hanging-wall subsidence increases as the dip of the fault decreases (Gibson et al., 1989). For large faults, footwall uplift is a consequence of displacement geometry plus isostatic effects (Jackson and McKenzie, 1983). Isostasy is not likely to be responsible for the footwall uplift observed on meter-scale and smaller normal faults.

In addition to variations in fault displacement along strike, displacement also decreases with distance normal to the fault surface, resulting in a reverse-drag geometry in both the hanging wall and footwall (Figure 1d) (Barnett et al., 1987). This geometry is a manifestation of the elastic and flexural (for large faults) response to faulting (see review in Roberts and Yielding, 1994). The distance from the fault at which fault displacement is negligible is known as the reverse-drag radius, which increases with increasing displacement (Gibson et al., 1989). Along any given profile normal to the strike of the fault, displacement is greatest at the fault surface, generally near the center of the fault, and decreases toward the fault tips and away from the fault itself. For isolated blind normal faults, this displacement geometry results in deformation of units in the volume surrounding the fault (Muraoka and Kamata, 1983; Barnett et al., 1987). There are four quadrants of deformation, two of which are dilational and two of which are contractional (Figure 1d). This deformational geometry probably affects permeability and porosity within the faulted volume (Barnett et al., 1987).

Within the last decade, considerable attention has been focused on the scaling relationship

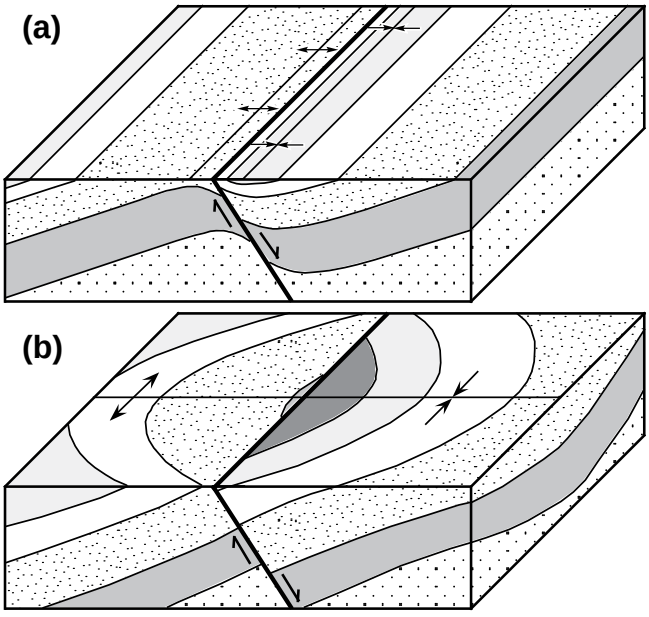

Figure 2—Idealized geometry of longitudinal (a) and transverse (b) folds.

between fault length and displacement. Building on the work of Elliott (1976), Watterson (1986) documented a positive relationship between fault length and displacement, and interpreted these results to indicate that faults grow in length as displacement accrues. The general scaling relation is $D = cL^n$, where D is displacement, c is a constant related to rock properties, L is length, and n is some exponent. Considerable debate surrounds the value of n; reported values range from 2 (Watterson, 1986; Walsh and Watterson, 1988) to 1.5 (Marrett and Allmendinger, 1991; Gillespie et al., 1992; Walsh and Watterson, 1992) to 1 (Cowie and Scholz, 1992a, b; Dawers et al., 1993; Young et al., 1995). Although the value of n affects the manner in which faults grow through time (Schlische, 1991; Schlische and Anders, in press), controversy about its exact value, if there is a unique value, does not change the fact that faults increase in length through time and that associated folds must change through time as well.

Normal fault systems on a variety of scales commonly consist of multiple fault segments (e.g., Schwartz and Coppersmith, 1984; see recent reviews by Gawthorpe and Hurst, 1993; Anders and Schlische, 1994; Davison, 1994; Childs et al., 1995; Schlische and Anders, in press). Individual segments of the fault system commonly exhibit the same displacement geometry as isolated normal faults (Dawers and Anders, 1995), although displacement gradients may be higher near segment boundaries (Peacock and Sanderson, 1991). Summing of displacements of individual faults commonly results in a displacement profile for the entire fault system that resembles the displacement profile of an isolated fault (e.g., Walsh and Watterson, 1991; Trudgill and Cartwright, 1994; Dawers and Anders, 1995), suggesting that the faults are kinematically linked and that the fault system evolved through the growth and linkage of originally isolated fault segments (Anders and Schlische, 1994). A very common type of fault linkage involves overlapping faults in which displacement is transferred from one fault to another via a zone of ductile deformation termed a "relay ramp" (Larsen, 1988; Peacock and Sanderson, 1991; Trudgill and Cartwright, 1994). Segment boundaries may be recognized by overlapping faults, fault offsets, significant changes in fault strike, reduced displacement, and differences in the age of faulting on either side of the segment boundary (e.g., Zhang et al., 1991).

Roberts and Yielding (1994) recognized three broad types of normal faults. (1) Small normal faults are confined entirely within the seismogenic layer; these are mostly planar but may exhibit changes in geometry as the faults pass through different lithologies (Peacock and Zhang, 1993). (2) Large normal faults penetrate the entire seismogenic layer, are planar with moderate dip angles (Stein and Barrientos, 1985; Jackson, 1987; Jackson and White, 1989), and are commonly associated with half-graben–type sedimentary basins (e.g., Rosendahl, 1987); flexural effects of faulting, sedimentation within the hanging-wall basin, and erosion of the uplifted footwall are important (e.g., Jackson and McKenzie, 1983; Stein et al., 1988). (3) Gravity-driven normal faults typically form within thick, usually regressive sedimentary sequences (passive margins, deltas); are commonly strongly listric and detached in weak, commonly overpressured sedimentary intervals; and create growth structures (e.g., Shelton, 1984).

FAULT-RELATED FOLDS IN EXTENSIONAL SETTINGS

The majority of folds in extensional tectonic environments are associated with normal fault systems. Longitudinal folds have hinges that are parallel or subparallel to the strike of the fault (Figure 2a), and are best observed in sections perpendicular to the fault. Transverse folds have hinges that are perpendicular and subperpendicular to the strike of the fault (Figure 2b), and are best observed in sections parallel to the fault. Transverse folds are commonly elongated parallel to the fault; the term transverse only strictly applies to the orientation of the hinge with respect to the

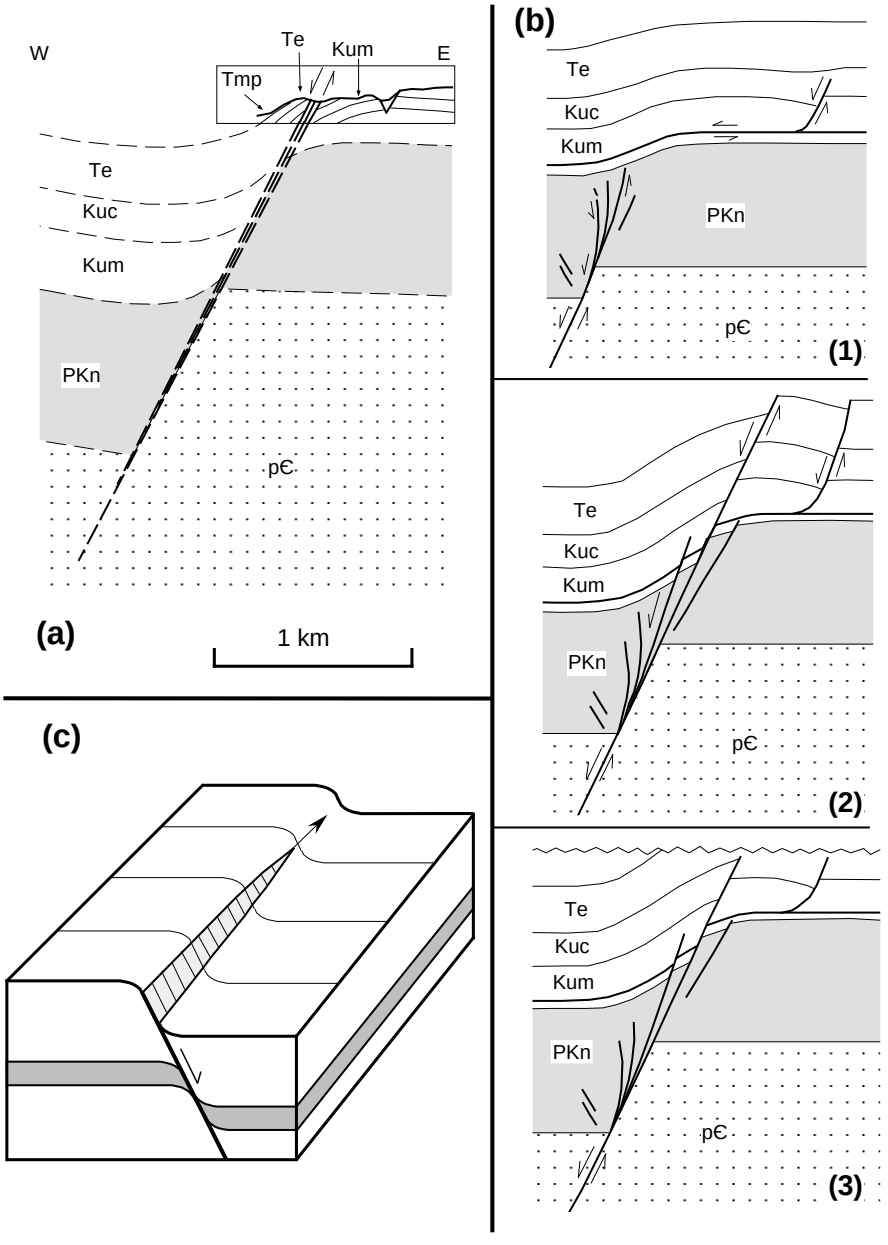

Figure 3—(a) Drag (forced) folds and associated basement-penetrating normal fault zone from the eastern El-Qa plain, Gulf of Suez. Box shows outcrop data. p€ = Precambrian basement; PKn = Nubia Sandstone (Carboniferous–Upper Cretaceous); Kum = Upper Cretaceous limestone and shale; Kuc = Upper Cretaceous–Paleocene shale and limestone; Te = Eocene limestone; and Tmp = Miocene–Pliocene units. Modified from Withjack et al. (1990). (b) Idealized cross sections illustrating evolution of forced folds in the Gulf of Suez as a result of upward fault propagation. Modified from Withjack et al. (1990). (c) Fault-propagation fold associated with lateral migration of fault tip. Modified from Walsh and Watterson (1987).

fault. Other folds are possible in extensional settings, but these typically are associated with strike-slip movement or later compressional events.

Longitudinal Folds

Drag Folds

Drag folds are longitudinal folds that are generally restricted to the region immediately adjacent to the fault surface (Figure 2a). Synclines form in the hanging walls of normal faults; anticlines are found in the footwalls. Drag folds form as a result of the lateral and upward propagation of faults (a consequence of fault growth) into regions that have been monoclinally flexed at the fault tips (Figure 3) (e.g., Hancock and Barka, 1987; Walsh and Watterson, 1987). Thus, drag folds may be considered fault-propagation folds (see Mitra, 1993). Drag folds may also form as a result of frictional drag along the fault surface (e.g., Hatcher, 1994). Unfaulted folds at the tips of normal faults are termed "forced folds" by Withjack et al. (1990). Drag and forced folds are common in the Gulf of Suez (Figure 3a, b) (e.g., Robson, 1971; Withjack et al., 1990), the Norwegian margin (Withjack et al., 1989), and the Rhine graben (Laubscher, 1982). Drag folds and related folds

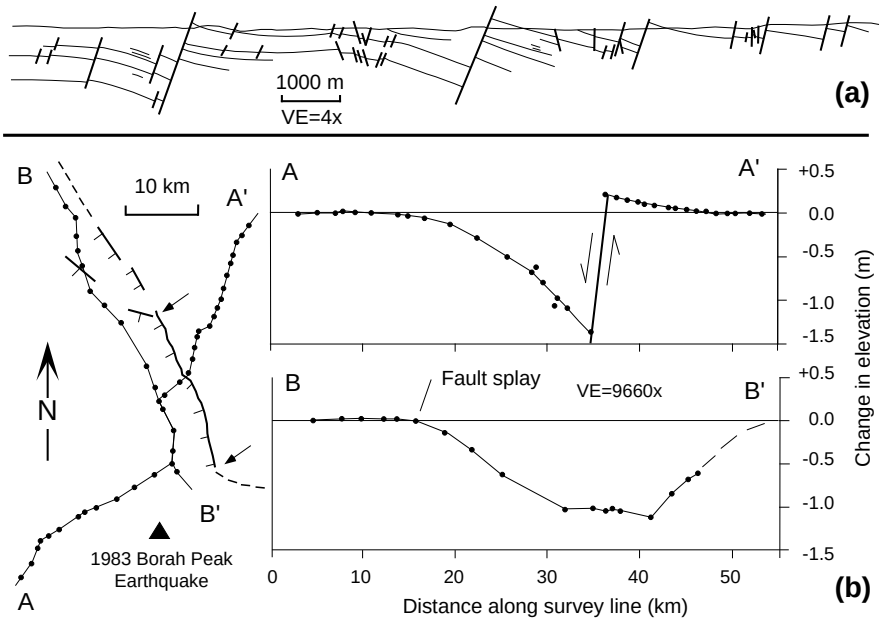

Figure 4—(a) Reverse-drag folds in both hanging walls and footwalls of normal faults within coalfields of the Dudley basin, Australia. Modified from Barnett et al. (1987). (b) Changes in ground-surface elevation perpendicular and parallel to the Lost River fault system, Idaho, following the 1983 Borah Peak earthquake. Dots indicate stations along survey transects. Compare the geometry in cross section AA′ with that shown in Figure 1d, and the geometry in cross-section BB′ with the hanging-wall cutoff in Figure 1c. Modified from Barrientos et al. (1987).

may form adjacent to all three major types of normal faults previously discussed.

Reverse-Drag Folds

As the name implies, reverse-drag folds have the opposite geometry of drag folds in that they form hanging-wall anticlines and footwall synclines (Figure 4a). In contrast to drag folds, reverse-drag folds are more areally extensive. As noted previously, reverse-drag folds are a manifestation of the decrease in displacement with distance from the fault surface (Figure 1d), which is an elastic and, in some cases, flexural response to faulting. Reverse-drag radius increases with fault displacement. As faults grow in size through time, the associated folds should grow in width and amplitude as well. In general, the amplitude of hanging-wall reverse-drag anticlines is higher than the amplitude of footwall reverse-drag synclines (Figure 4a). Drag folds may be superimposed on reverse-drag folds, resulting in composite folds. Reverse-drag folds are typically associated with small and large faults. The reverse-drag geometry is also produced by seismic slip on normal faults (Figure 4b; Stein and Barrientos, 1985).

Rollover Folds Associated with Detached Normal Faults

Rollover folds (Figure 5) are common within thick sedimentary successions associated with passive margins, notably the Gulf Coast region and the Niger delta (see references and examples in Bally et al., 1981; Shelton, 1984; and Roberts and Yielding, 1994). Rollover folds form as a result of movement on concave-upward (listric) faults and are thus the extensional equivalents of fault-bend folds (Figure 5a, b). Movement on these faults creates a potential void between the hanging wall and the footwall; the hanging wall then collapses into the void (Figure 5a). In reality, a void is never produced because fault movement and hanging-wall deformation occur simultaneously. Because the faults associated with rollover folds form in non-lithified materials, which have little strength, footwall folds similar to those associated with reverse drag are generally absent (Roberts and Yielding, 1994), but footwall deformation may occur in response to deformation of underlying shales (A. W. Bally, 1995, personal communication).

The geometry of a rollover fold is controlled by the shape of the fault surface and the mechanism by which the hanging wall deforms to fill the potential void. Deformation mechanisms include vertical simple shear (e.g., Gibbs, 1983), inclined simple shear (e.g., White et al., 1986), and flexural slip (Davison, 1986). The type of deformation mechanism may depend on the lithologies being affected (Rowan and Kligfield, 1989). Kink-type folds are produced where the listric fault consists of planar segments (Figure 5b; Groshong, 1989; Xiao and Suppe, 1992). This fault geometry may result from differential compaction (Shelton, 1984; Davison, 1987) or as a result of refraction as the fault passes through layers of differing pore-fluid pressures and mechanical properties (e.g., Murray, 1961; Bradshaw and Zoback, 1988).

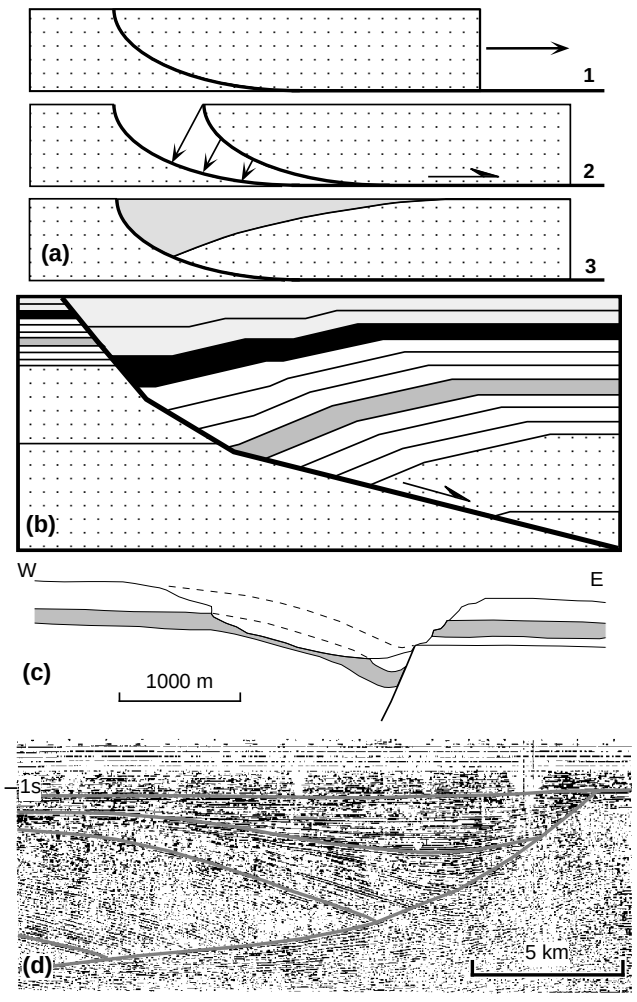

Figure 5—Rollover folds associated with movement on a smoothly curved listric fault (a) and a kinked fault (b) (modified from Xiao and Suppe, 1992). (c) Rollover and normal-drag folds in the hanging wall of the Big Springs fault, Arizona. Modified from Hamblin (1965). (d) Rollover fold associated with listric fault in the Bohai Gulf of northern China; note the drag fold adjacent to the normal fault. Modified from Zhang (1994).

Numerous "balancing" models have been proposed in the literature to reconstruct fault geometry based on the rollover shape or vice versa (see recent reviews by Dula, 1991; Withjack and Peterson, 1993; and Groshong, 1994). Some recent models have incorporated the effects of compaction (e.g., Rowan and Kligfield, 1989; White and Yielding, 1991), involved multiple faults (de Matos, 1993), and extended the reconstruction to three dimensions (e.g., Kerr et al., 1993). Roberts and Yielding (1994) have cautioned that such balancing techniques should only be used in reconstructing the geometry of detached normal faults and should not be applied to basement-penetrating faults.

Given the geometric similarity, the terms "rollover" and "reverse drag" are used interchangeably in the literature. If a distinction is drawn, it is that rollover folds involve a reversal in dip direction, whereas reverse drag involves a steepening of dip (e.g., Shelton, 1984). Recall that reverse drag (as used in this paper) is the elastic-flexural response to tectonic faulting in lithified rock, whereas rollover folds are associated with gravity-driven listric faults. Given the fundamental mechanical difference between these two types of faulting, I recommend that the terms not be used interchangeably and that rollover only be applied to longitudinal hanging-wall anticlines associated with gravity-driven listric faults, even if there is not a dip reversal.

The presence of rollover folds is a good indicator that the associated fault is listric (Figure 5c) (e.g., Hamblin, 1965). However, as already noted, rollover and reverse-drag anticlines have nearly identical geometries. Reverse-drag anticlines may be mistakenly interpreted to be rollover folds, and the associated fault may be erroneously inferred to be listric. As originally noted by Barnett et al. (1987), the presence of reverse-drag folds does not imply the presence of listric faults. In fact, most reverse-drag folds are associated with planar or only mildly listric faults. An additional complication is that the listric appearance of faults on seismic reflection profiles may be caused by velocity pull-ups (Withjack and Drickman Pollock, 1984). Distinguishing between rollover and reverse-drag folds relies on the following: (1) rollover folds are to be expected in thick sedimentary successions in association with detached normal faults; (2) reverse-drag folds are present in both the footwall and hanging wall, whereas rollover folds are generally found only in the hanging wall. It may be necessary to construct vertically exaggerated profiles to identify footwall reverse drag, which is of smaller amplitude than hanging-wall reverse drag for faults that intersect the Earth's surface.

In some cases, seismic data show folds superimposed on rollover folds (Figure 5c, d). Gibson et al. (1989) suggested that these drag-like folds formed as a result of differential compaction. According to Xiao and Suppe (1992), drag-fold–like structures may also be produced by movement along convex-upward normal faults.

Transverse Folds

All types of transverse folds result from along-strike variations in fault displacement, which is a scale-invariant feature of normal faults. Thus,

transverse folds also exist on a variety of scales. The style of transverse folding depends largely on the geometry of the normal fault system (isolated fault vs. segmented fault system).

Folds Associated with an Isolated Fault

In the hanging wall of a single isolated fault, along-strike variations in fault displacement produce a broad, elongated syncline that plunges toward the fault (Figure 2b); for a large isolated basin-bounding fault, the syncline defines a sedimentary basin (Figure 6a). A broad, elongated anticline, plunging away from the fault, is present in the footwall (Figures 2b, 6a). The fold hinges for both folds should be collinear and are located in the region of maximum fault displacement (Figures 2b, 6a). The amplitude of the syncline is commonly greater than the amplitude of the anticline, as hanging-wall displacement is commonly greater than footwall displacement. As a result of fault and basin growth, the amplitude of the folds and the width of the folds increase through time, although the hinge lines are likely to remain relatively fixed (Figure 6a). Hinge-line migration may occur if the area of maximum displacement shifts position through time, which might be recognizable by the presence of curved axial surfaces (Schlische and Anders, in press).

Folds Associated with Segmented Fault Systems

Segmented fault systems are commonly associated with multiple displacement minima and maxima (Figure 6b–e). For the hanging wall of the fault system, synclines form at local displacement maxima, typically located at or near the centers of the fault segments; anticlines form at local displacement minima, typically located near fault segment boundaries (Figure 7a). The synclines are considerably wider than the anticlines, which are commonly associated with relay ramps between overlapping fault segments. The concept of relay ramps and displacement transfer between overlapping faults can largely be traced to Larsen's (1988) study of the geometry of segmented normal fault systems in Permian rifts of Greenland (Figure 7b), where multiple transverse folds are found in the hanging wall (Figure 7c).

In the footwall of a segmented fault system, anticlines form at local displacement maxima, which, when present, are typically located at or near the centers of fault segments; synclines form at local displacement minima, which, when present, are typically located at fault segment boundaries. The extent to which transverse folds are developed in the footwall and the hanging wall depends on the number of active fault segments, the stage in the evolution of the fault system, and the nature of the fault segment geometry. According to Anders and Schlische (1994) and Schlische and Anders (in press), fault geometry for multiple-segment fault systems can be classified as (1) nonoverlapping, (2) closely overlapping, and (3) widely overlapping. For each broad class, additional geometries are possible depending on whether the faults dip synthetically or antithetically. The evolutionary models for the specific cases shown in Figure 6, which are based on Schlische and Anders (in press), apply to basin-scale fault systems. However, as noted previously, the displacement geometries are scale invariant.

In the case of nonoverlapping synthetic faults, isolated synclinal subbasins originally form in the hanging wall (Figure 6b, stage 1). Footwall uplift profiles define broad anticlines associated with the isolated fault segments. As displacement accrues, the fault tips propagate laterally, and the fault segments eventually link together. At this stage, the synclinal subbasins are separated by a transverse high located in the region of low displacement where the faults linked together (Figure 6b, stage 2); the opposite fold geometry exists in the footwall. Eventually, displacement must increase in the zone of linkage so that the maximum displacement on the fault system conforms to length-displacement scaling relationships (Anders and Schlische, 1994). Thus, the transverse high gradually subsides, eventually resulting in a single elongated syncline in the hanging wall and a single elongated anticline in the footwall (Figure 6b, stage 3).

The initial geometry of the structures associated with closely overlapping synthetic faults is similar to that of nonoverlapping synthetic faults (Figure 6c, stage 1). As the fault tips propagate laterally and begin to overlap, a transverse anticline forms and separates two synclines in the hanging wall (Figure 6c, stage 2); a transverse syncline forms in the footwall in the area of overlap. According to Anders and Schlische (1994), the transverse anticline in the hanging wall will persist as long as multiple fault segments are coevally active so that slip is distributed on multiple faults, thus reducing the amount of hanging-wall subsidence (Figure 6c, stage 3). If the overlapping faults physically link together, then the transverse high will eventually subside. Anders and Schlische (1994) suggested that the footwall elevation low will gradually disappear, even if multiple overlapping fault segments remain active (Figure 6c, stage 3). This is because the footwall elevation profile reflects the total displacement on the fault system (particularly the displacement at depth), whereas the near-surface displacement on the nearest fault segment determines the depth of the hanging-wall basin.

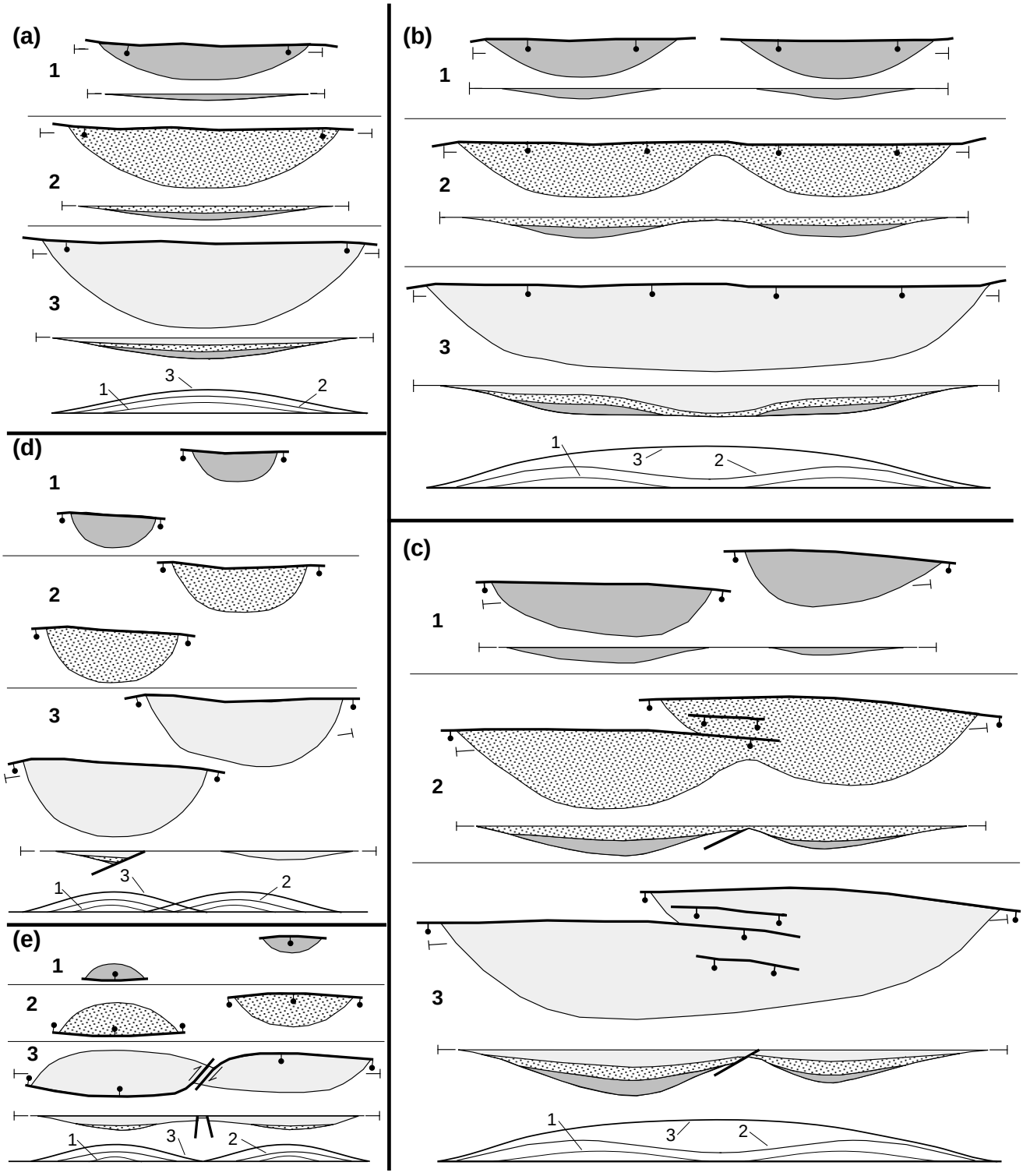

Figure 6—Evolution of extensional basins resulting from fault growth. Each panel shows three stages in the hanging-wall evolution of an extensional basin or subbasin system; ball-and-bar symbols indicate normal faults. Longitudinal sections shown for each stage in basin evolution [except stages 1 and 2 for (d) and (e)]. The lower diagram in each panel shows geometry of footwall uplift after each of the three stages. (a) Single fault; (b) nonoverlapping synthetic fault segments; (c) closely spaced overlapping synthetic fault segments; (d) widely spaced overlapping synthetic fault segments; and (e) antithetic fault segments. Simplified from Schlische and Anders (in press).

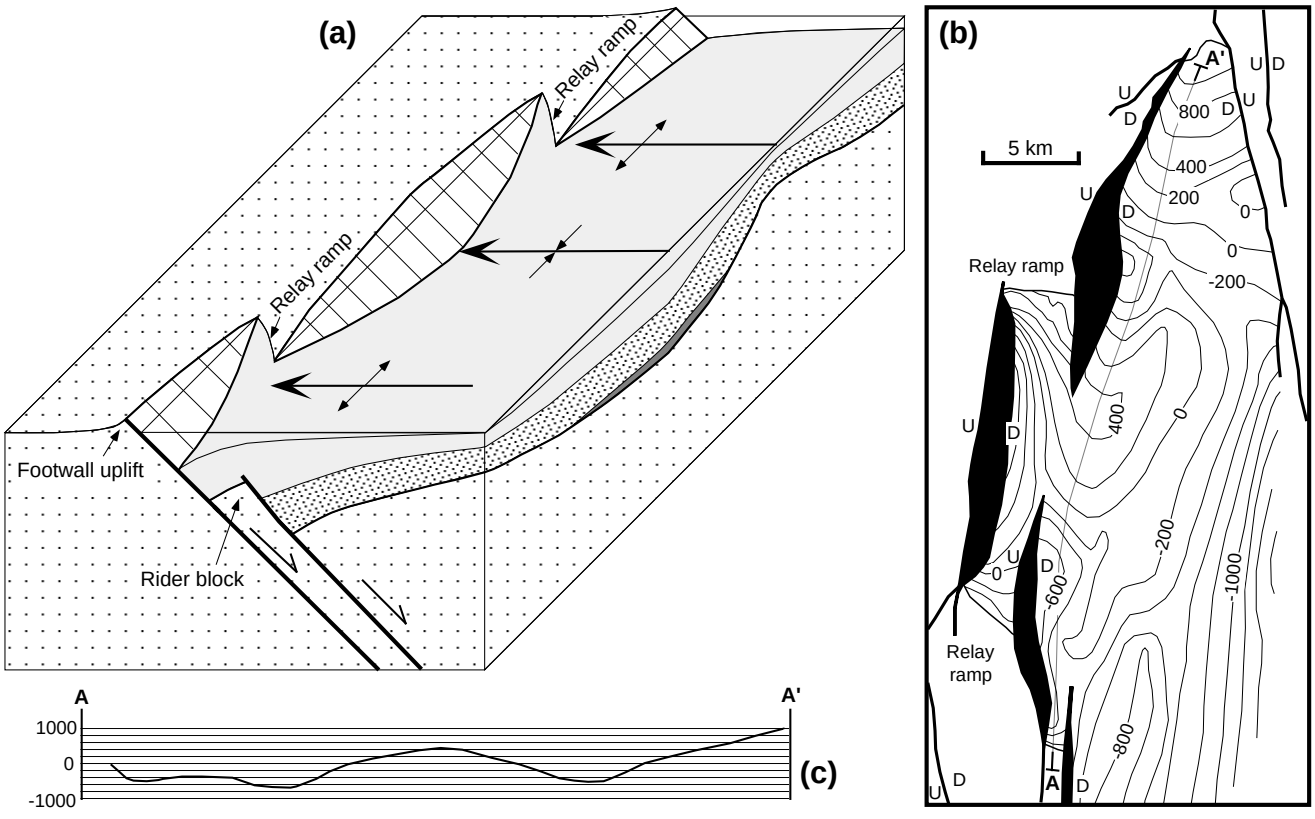

Figure 7—(a) Geometric relationships among a segmented normal fault system, relay ramps, transverse folds, and rider blocks. Simplified from Schlische (1993). (b) Structure-contour map of the top of basement (datum is mean sea level) within a Permian rift basin, Greenland. Note relay ramps between offset fault segments, basement highs (transverse anticlines) at fault segment boundaries, and basement lows (transverse synclines) near the centers of fault segments. Adapted from Larsen (1988). (c) Longitudinal profile of top of basement along section AA′ shown in (b).

In the case of widely spaced overlapping synthetic faults, originally isolated synclinal subbasins never merge during fault-tip propagation (Figure 6d). Each fault segment is associated with its own anticlinal footwall uplift geometry. However, the summed footwall uplift profile resembles that of a single continuous fault.

The relay geometry of synthetic overlapping faults may not persist indefinitely (Peacock and Sanderson, 1991; Childs et al., 1995). Relay zones are commonly breached by faults that connect the main fault segments. This may account for the dogleg or zig-zag geometry of some normal fault systems (e.g., Harding, 1984).

An example of the evolution of one type of antithetic fault system is shown in Figure 6e. Each fault segment produces an originally isolated synclinal subbasin. As the tips propagate, the faults curve toward one another to prevent interference. Reduced displacement at the fault tips coupled with greater strike slip on fault segments oblique to the extension direction result in reduced subsidence in the area of fault overlap, forming a transverse anticline. If the faults did not curve in this manner, a transfer fault would need to form between them. The footwall fold pattern consists of isolated anticlines; this geometry persists through time. Additional examples of the geometry of antithetic fault systems are provided by Morley et al. (1990).

Examples of Basin-Scale Transverse Folds

The Beaverhead and Lost River fault systems of Idaho (northern Basin and Range) each consist of six fault segments (Anders and Schlische, 1994; Figure 8a). Segment boundaries marked by closely overlapping faults (shaded) are associated with hanging-wall highs (intrabasin highs) manifested as Bouguer anomaly highs (indicating shallower depth to basement). In the regions of overlap, there is no associated footwall elevation low. Rather, the anticlinal footwall uplift profiles resemble those of a single fault, suggesting that all of the fault segments are kinematically linked. The geometries depicted in Figure 8a

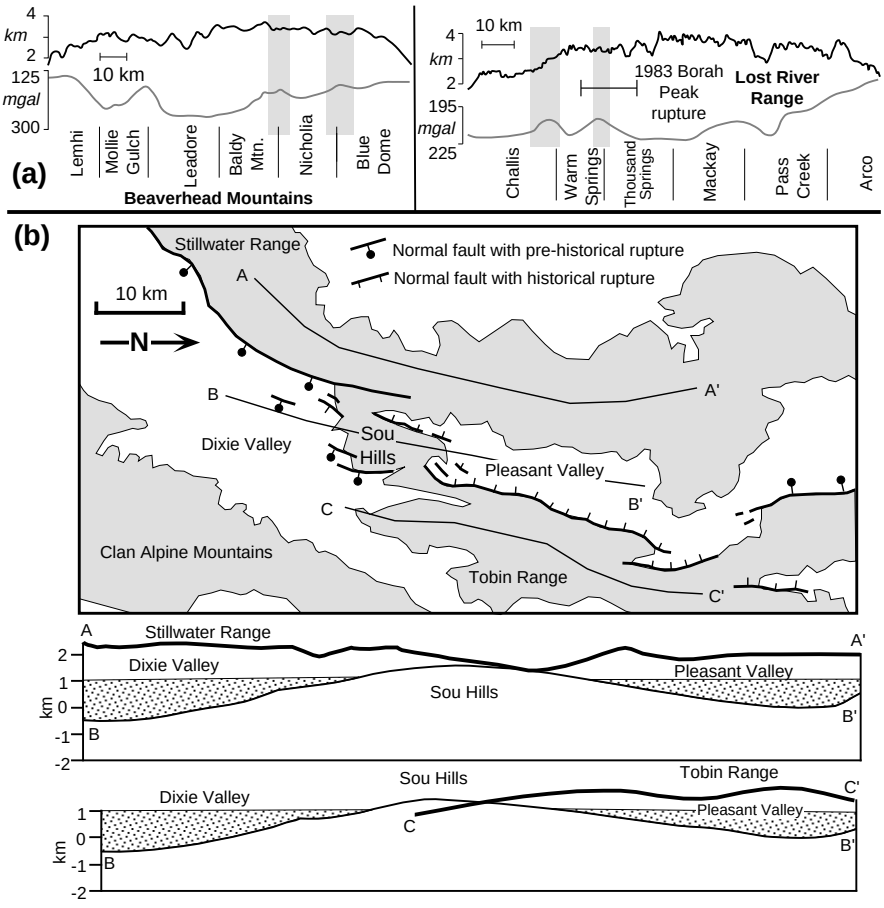

Figure 8—(a) Transverse folds associated with recent normal fault systems in the Basin and Range. Range-crest longitudinal footwall elevation profile and longitudinal Bouguer gravity anomaly profile (a proxy of hanging-wall subsidence) for the Beaverhead and Lost River fault systems, Idaho; the names of fault segments and segment boundaries are indicated. Intrabasin highs are not associated with footwall elevation lows at the shaded segment boundaries. Modified from Anders and Schlische (1994). (b) Upper panel: geologic map of the Dixie Valley–Pleasant Valley fault system. Modified from Zhang et al. (1991). Lower panel: longitudinal profiles of footwall uplift and hanging-wall subsidence along transects indicated in the upper panel. Modified from Jackson and Leeder (1994).

correspond to stage 3 in the evolution of a closely overlapping synthetic fault system (Figure 6c).

The Dixie Valley–Pleasant Valley fault system of Nevada is an example of an overlapping antithetic fault system. Dixie Valley and Pleasant Valley are two synclinal subbasins associated with the southeast-dipping Dixie Valley fault and the northwest-dipping Pleasant Valley fault, respectively (Figure 8b). The Sou Hills is an anticlinal high (accommodation zone) formed in the area where the two major fault systems overlap (Fonseca, 1988; Gawthorpe and Hurst, 1993; Schlische and Anders, in press). The Sou Hills area is also associated with footwall elevation lows in the Stillwater and Tobin ranges (Jackson and Leeder, 1994).

In the Triassic–Jurassic rift system in eastern North America (Figure 9), the Newark and Culpeper basins are relatively simple basins, consisting of elongated synclines in longitudinal section, although this simple geometry is complicated by intrabasinal normal faults and higher amplitude folds along the border fault system. In the Newark basin, strata thicken and lacustrine facies deepen toward the hinge of the basin-scale syncline (Schlische, 1992). The Hartford-Deerfield and Deep River basins consist of multiple synclinal subbasins separated by intrabasin highs, marking regions where originally isolated subbasins grew together (Schlische, 1993). In the Hartford-Deerfield basin, strata thicken toward the hinges of the synclinal subbasins, and paleocurrents within fluvial units are directed away from the intrabasin high between the two subbasins (Schlische, 1993).

Fault-Displacement Folds

Fault-displacement folds are transverse folds of smaller scale than those discussed in the previous section. In some cases, these folds are associated with segmented fault systems similar in geometry but smaller in length of segments than those described (e.g., Figure 7b). In other cases, the folds are not associated with an obvious or heretofore mapped segmented fault system. Nonetheless, the folds have a geometry similar to those that are definitely associated with segmented faults, and thus they are also likely related to along-strike variations in fault displacement.

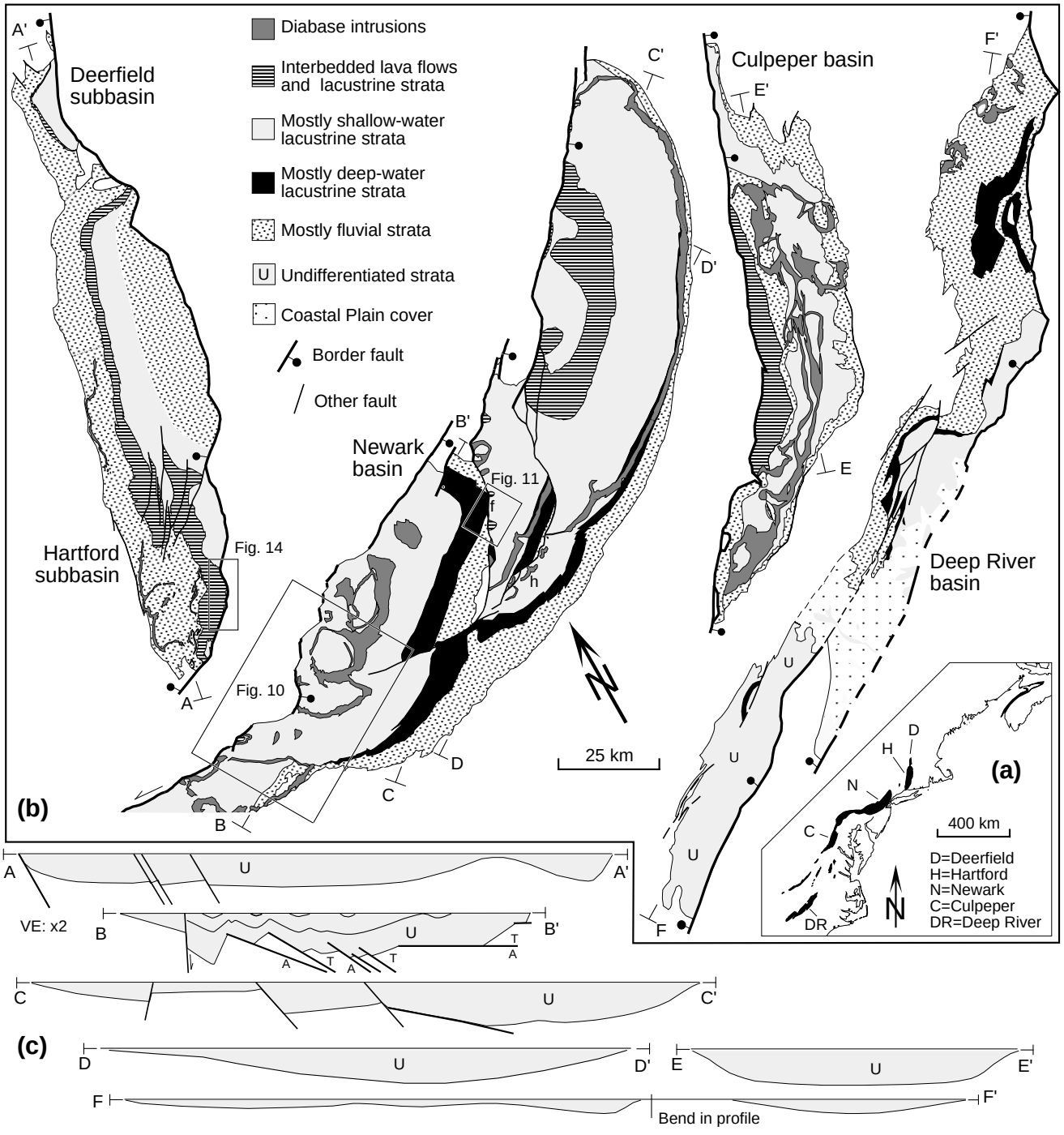

Figure 9—Simplified geologic maps (b) and schematic longitudinal cross sections (c) of selected Mesozoic rift basins of eastern North America (a). f = Flemington fault; h = Hopewell fault; A = motion away from reader; T = motion toward reader. Modified from Schlische (1992, 1993).

Transverse folds are present along the border fault system in the northeastern part of the Newark basin (Figure 9b). These folds decrease in amplitude away from the fault, clearly do not affect the entire width of the basin, and are not associated with any obvious or mapped fault segmentation. In the southwestern part of the basin, transverse folds are also well developed (cross section BB′ in Figure 9c), but

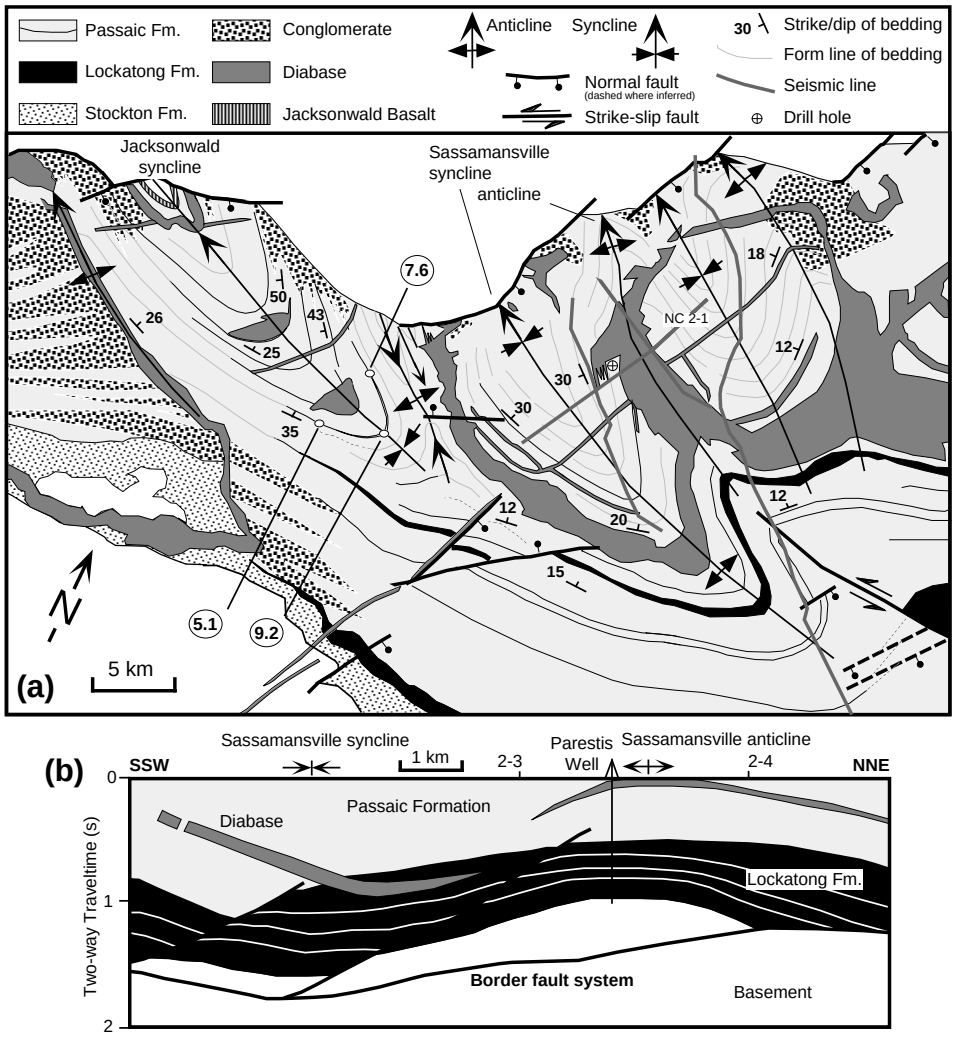

Figure 10—(a) Geologic map of the southwestern Newark basin (see Figure 9b for location) showing transverse folds associated with a segmented fault system and location of seismic lines studied by Reynolds (1994). Circled numbers indicate thicknesses of marker unit in meters. Modified from Schlische (1992). (b) Geologic interpretation of longitudinal seismic line NC 2-1. Modified from Reynolds (1994).

in this case there is a clear association between the folds and a highly segmented border fault system (Figure 10a). The local and regional geometry of the folds is most compatible with normal faulting (see Schlische, 1992, for further discussion).

Outcrop and seismic reflection data from the Jacksonwald-Sassamansville area in the southwestern Newark basin constrain the timing of deformation. In the Jacksonwald syncline, stratigraphic marker beds are thicker in the hinge than along the limbs (Figure 10a) (Schlische, 1992). Reynolds (1994) analyzed a grid of seismic reflection profiles (provided by North-Central Oil and Exxon Corporation) in the southwestern Newark basin. Line NC 2-1 is oriented subparallel to the border fault system (Figure 10b). Reynolds' interpretation shows that synrift strata and the top of basement are concordantly folded. Although the border fault system is not planar, its irregularities do not systematically correlate with the overlying folds. As constrained by the seismic data and the Parestis well, the Lockatong Formation is thinnest along the crest of the Sassamansville anticline and thickens into the flanking synclines (Figure 10b). Both studies clearly indicate syndepositional folding.

Transverse folds are also well developed along the Flemington and Hopewell intrabasinal normal fault systems (f and h in Figure 9b). The amplitude of folding decreases with distance from the Flemington fault system in the hanging wall (Figure 11a). No folds of a scale similar to those in the hanging wall are present in the footwall. Stratigraphic data from marker beds that have been traced across the folds (Olsen et al., in press) indicate that units thicken and lacustrine facies deepen away from the anticlinal hinge (Figure 11b), strongly suggesting syndepositional folding. A drag fold is present near the southwestern end of the fault shown in Figure 11a.

As displacement increases on faults or fault segments, transverse folds must increase in amplitude.

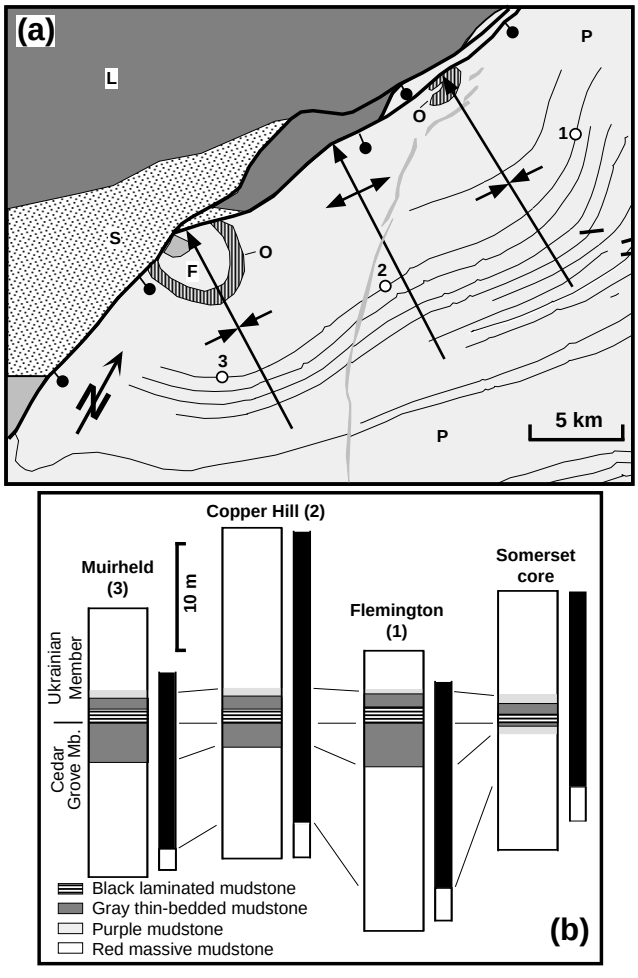

Figure 11—(a) Geologic map of a part of the Flemington intrabasinal fault system of the central Newark basin (see Figure 9b for location), with transverse folds in the hanging wall. F = Feltville Formation; L = Lockatong Formation; O = Orange Mountain Basalt; P = Passaic Formation; S = Stockton Formation. Thin black lines are marker beds consisting of deeper water lacustrine strata. (b) Measured stratigraphic sections [see (a) for locations] and paleomagnetic polarity stratigraphy (black is normal, white is reversed) of top of the Cedar Grove Member and base of the Ukrainian Member, showing thinning toward the anticlinal hinge and thickening toward the synclinal hinges. Modified from Olsen et al. (in press).

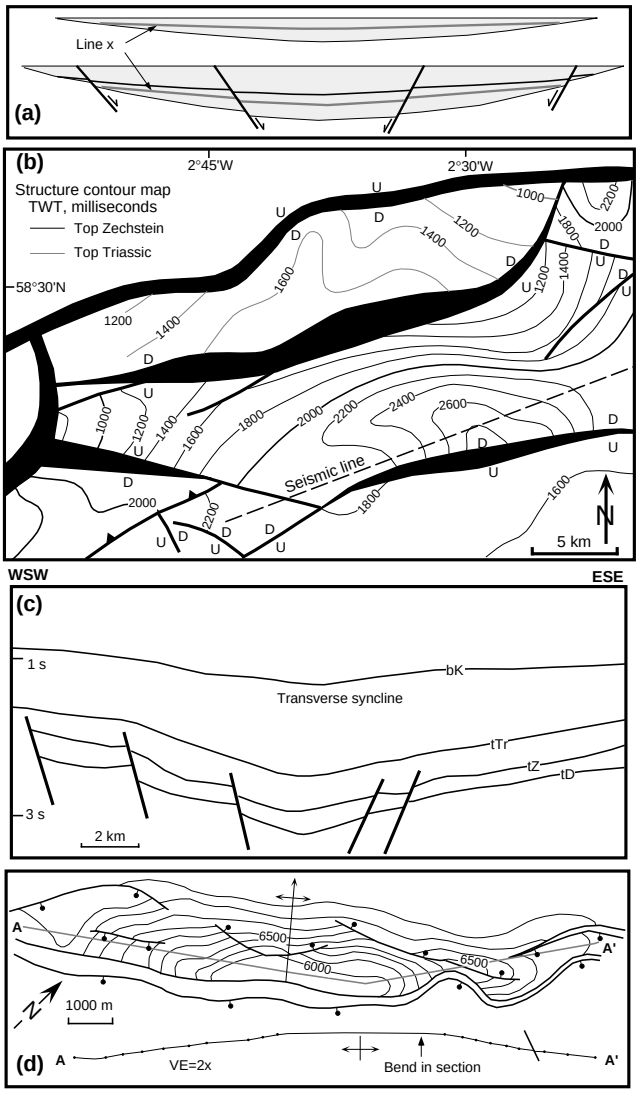

Figure 12—(a) Changes in bed length during fault-displacement folding accommodated by transverse normal faulting. (b) Structure contour map of a part of the North Sea, with faulted transverse syncline imaged on seismic reflection profile (c). tD = top Devonian; tZ = top Zechstein; tTr = top Triassic; bK = base Cretaceous. Map simplified from and original seismic data presented by Roberts et al. (1990). (d) Footwall anticline associated with normal fault system (ball-and-bar symbols) in the Beatrice field, North Sea. Contours are depth in feet to the upper surface of the reservoir unit. Modified from Linsley et al. (1980).

Consequently, bed lengths of units deformed by the folding must increase through time (Figure 12a). Transverse folding of this type therefore leads to the formation of fold-parallel (fault-perpendicular) extensional structures, such as joints, normal faults, and dikes. Such relatively small-scale accommodation structures have been imaged on a seismic reflection profile of a transverse fold in the North Sea (Figure 12b, c) (Roberts et al., 1990). The normal faults form a conjugate system, dipping toward the locus of greatest subsidence, and are restricted to older horizons that have been downwarped the most. Strata thicken toward the center of this syndepositional structure. [It should be noted that Roberts et al. (1990) ascribed this fold to strike slip, but its geometry is very similar to other transverse folds described in this report, and is probably a fault-displacement

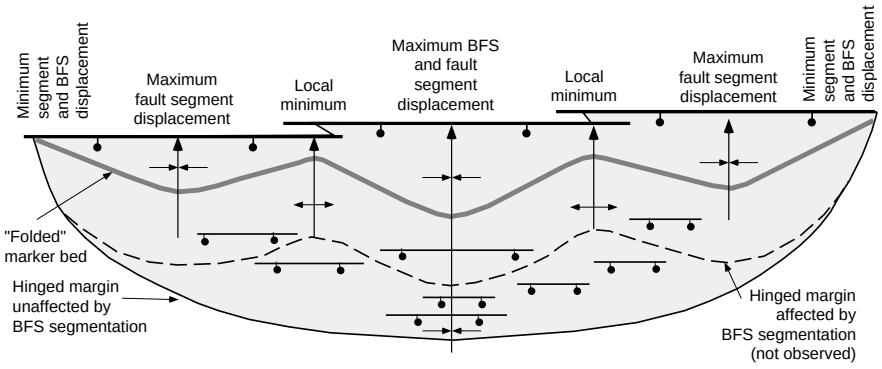

Figure 13—Hierarchy of transverse folds associated with extensional basins. BFS refers to border fault system. Ball-and-bar symbols denote normal faults. See text for discussion.

fold (A. M. Roberts, 1995, personal communication).] In the southwestern Newark basin (Figure 10a), a large northwest-striking subvertical dike subparallels the hinge of the Jacksonwald syncline, and is likely a fold-parallel extensional structure that accommodated progressive transverse folding.

A hierarchy of fault-displacement folds is present in the Newark basin and presumably other basins as well. The largest scale fold is associated with the basin itself (Figures 9b and 13); this suggests that on the largest scale, the basin appears to be bounded by a single continuous border fault, although the border fault is mapped as consisting of numerous fault segments. Superimposed on the basin-scale fold are transverse folds associated with the segmented border fault (Figure 13). Their effects are relatively localized; the hinged margin is clearly not affected by these folds (Figure 13). The distance of the hinged margin from the border fault system (i.e., the width of the basin) is a proxy of the total amount of extension experienced on the border fault system and the intrabasinal faults, both mapped and hidden. As noted by Marrett and Allmendinger (1992) and Walsh et al. (1991), hidden (i.e., small) faults commonly account for significant amounts of extension. Although each fault segment has a local displacement minimum at a fault segment boundary, resulting in the formation of an anticline in the immediate vicinity of the segment boundary, the sum of the displacements on the overlapping faults and any other faults balances for the localized deficits on any individual fault (Figure 13). To produce the overall synclinal geometry of the Newark basin, the central fault segments must have greater displacement than the distal segments. In addition, intrabasinal faults are concentrated in the central part of the Newark basin (Figure 9b) and may contribute to the greater width of the basin in that area.

Fault-Line Deflection Folds

Fault-line deflection folds were first described by Wheeler (1939). These transverse folds are associated with nonplanar fault surfaces. Synclines form at recesses (convex toward the footwall) in the fault surface, whereas anticlines form at salients (convex toward the hanging wall) (Figure 14). The amplitude of folding decreases away from the fault-line deflection, which is attributable to an "evening-out" effect with distance from the fault. The fault-segmentation model for the formation of transverse folds and the fault-line deflection model are not necessarily mutually exclusive because many segment boundaries (areas of displacement deficits) are marked by salients in the fault surface (e.g., Machette et al., 1991) and thus transverse anticlines. Dog-leg or zig-zag-type fault systems resulting from breached relay zones of overlapping faults may also be associated with fault-line deflection folds.

Fault-line deflections (undulations) have also been reported from several detachment faults in the southwestern United States (e.g., Davis and Lister, 1988). These folds have wavelengths of several tens of meters to hundreds of meters; the axes of these folds are subparallel to the slip direction. Meter-scale structures on neotectonic normal faults are referred to as corrugations by Stewart and Hancock (1991).

Interference Folds

The folds described previously account for the vast majority of folds found in extensional settings, but there are some additional examples that are not easily classified as transverse or longitudinal. Interference folds form when one type of fold is superimposed on another; for example, longitudinal folds superimposed on transverse folds. Depending on the geometry of the superimposed folds, domes, basins, saddles, and culminations (Figure 12d) may be produced.

DISCUSSION

The majority of the folds described previously are related to (1) movement on normal faults, (2)

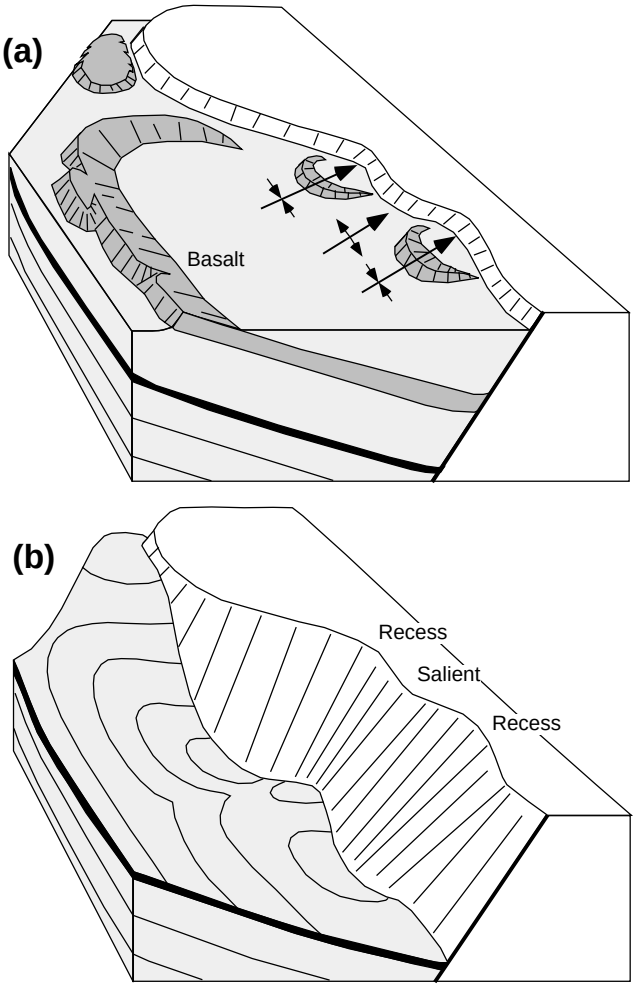

Figure 14—Transverse folds associated with fault-line deflections along the border fault system of the Hartford subbasin, Connecticut (see Figure 9b for location). Synclines form at recesses; anticlines form at salients. (a) Present-day geometry; (b) geometry with upper synrift units removed. Modified from Wheeler (1939).

growth and propagation of faults, and (3) displacement variations on normal faults and in the volume of rock affected by the faulting. Fault-related folds therefore form at the same time as the faults or, in the case of drag folds, immediately prior to faulting. Folds related to faults that intersect the free surface of the Earth are therefore expected to grow syndepositionally. Consequently, sedimentary units influenced by the folds will be thicker in the hinges of synclines and thinner or absent on the crests of anticlines. Sedimentary facies are expected to have been deposited in deeper water in the hinges of synclines; shallower water deposits are expected in the hinges of anticlines. Emergent footwalls may be sites of nondeposition or erosion. As faults or fault segments grow longer through time, most folds will also increase in size. During the growth and evolution of segmented basins, some structures might gradually be replaced by others (e.g., intrabasin highs gradually subsiding as multiple depocenters evolve into a single depocenter).

Within the hanging walls of normal fault systems, anticlines (intrabasin highs) form at fault segment boundaries. In the case of overlapping faults, these segment boundaries are commonly associated with relay ramps and, at least in the initial stages of fault linkage, zones of reduced footwall uplift (Figure 7a). Streams flowing off the uplifted footwalls commonly exploit these low points, and thus relay ramps serve as important conduits for transporting sediment from the footwall to the hanging wall (e.g., Leeder and Gawthorpe, 1987; Roberts et al., 1991; Gawthorpe and Hurst, 1993). At these input zones, sediments are expected to be somewhat coarser grained and may serve as potential reservoir rocks; e.g., sand bodies within the South Viking graben (Jackson and White, 1989) and Central graben (Roberts et al., 1991) of the North Sea. Such relay ramps are therefore important exploration targets; however, relay ramps themselves may be difficult to detect seismically, but the associated transverse anticlines may be easier to identify. As the fault system evolves, footwall elevation lows at some segment boundaries are gradually eliminated (see Figure 6c). In such cases, the supply of coarser clastics is shut off, and the older, coarser rocks may be buried by finer grained sediments that may serve as seals. This would form the ideal trap: coarser grained clastic rocks sealed by fine-grained rocks on an anticlinal structure, with hydrocarbons derived from the deep-water shales of adjacent synclines.

The wealth of folds and faults in extensional tectonic settings provides numerous structural traps. Footwall structural traps include drag folds, forced folds, and fault-propagation folds, which are associated with productive fields in, for example, the Sirte basin, Gulf of Suez, and the Viking graben (Harding, 1984). Footwall folds provide effective structural closure because displacement (uplift) is a maximum at the center of an associated fault segment and decreases toward the fault tip, and uplift decreases with distance from the fault. The fault itself or impermeable layers in the hanging wall may provide seals along the fault-bounded side of the trap. The Beatrice field in the North Sea is an excellent example of this type of structural trap (Figure 12d). Closure may be enhanced by the superposition of transverse anticlines and longitudinal drag folds. Folds associated with intrabasinal faults containing synextensional sedimentary deposits in the footwall are preferred to large border fault systems that typically lack synextensional deposits in the footwall.

Structural traps in the hanging walls of normal faults include the aforementioned fault-displacement anticlines associated with segmented fault systems and relay ramps and rollover folds (e.g., Shelton, 1984). Hanging-wall reverse-drag anticlines affecting units with regional subhorizontal orientation may not provide closure, especially if superposed transverse synclines create saddle structures. Closure may be possible if the regional dip is in the same direction as the dip direction of the fault. Interference folds, particularly domes and culminations, also may form structural traps.

In regions in which strata lack primary porosity and permeability, secondary fracture porosity is extremely important. Secondary structures associated with folds that may contribute to fracture permeability include (1) fold-parallel extensional structures that accommodate downwarping and upwarping associated with fault-displacement folds (Figure 12a), (2) fold-parallel faults and shear zones that accommodate reverse-drag and rollover folding, and (3) extensional structures in the lower footwall and upper hanging-wall quadrants associated with displacement fields on blind faults (Figure 1d).

Longitudinal folds, such as drag folds and rollover folds, have long been recognized as being associated with normal faults. One of the goals of this paper is to show that transverse folds are equally as common as longitudinal folds. Hopefully, the idealized models and examples of fault-associated folds presented in this paper will allow for augmented interpretations of seismic reflection profiles in areas of poor data quality.

SUMMARY AND CONCLUSIONS

(1) Characteristics of normal faults that influence associated folds include the following: maximum displacement occurs at the center of the fault and decreases toward the fault tips; displacement decreases with distance from the fault surface; faults increase in length as displacement increases; and fault systems are commonly segmented.

(2) Folds associated with normal faults can broadly be classified as fault-parallel (longitudinal folds) and fault-normal (transverse folds).

(3) Drag folds (including forced folds and fault-propagation folds) are longitudinal folds that form largely as a result of the growth of faults into regions of monoclinal folding at the tips of faults; synclines are present in the hanging wall; anticlines are present in the footwall. Such folds may also be produced by frictional drag and differential compaction.

(4) As defined in this paper, reverse-drag folds are longitudinal folds that are a manifestation of the elastic (and in some cases flexural) response to faulting that results in a decrease in displacement with distance from the fault; these folds consist of hanging-wall anticlines and footwall synclines.

(5) As defined in this paper, rollover folds are longitudinal folds that form as a result of movement on nonplanar (typically listric) faults in unlithified sediments in which movement is driven by gravity sliding. Anticlines form in the hanging wall; the footwall is generally unfolded. Although rollover anticlines are geometrically similar to reverse-drag anticlines, the causal mechanism is different. This geometry by itself cannot be used to infer the existence of listric faults. Balancing techniques used to infer fault geometry can only be used for rollover folds associated with gravity-driven faults.

(6) The majority of transverse folds form as a result of along-strike variations in fault displacement. In the hanging wall, synclines form near displacement maxima, typically at or near the centers of fault segments. Anticlines form near displacement minima, typically near fault segment boundaries. Synclines tend to be broader than anticlines. In the footwall, anticlines form at displacement maxima, and synclines form at displacement minima. The geometry of transverse folds is strongly influenced by the growth and linkage of fault segments.

(7) Fault-line deflection folds are transverse folds related to undulations on the fault surfaces, with synclines forming at recesses and anticlines forming at salients.

(8) Interference folds result from the superposition of longitudinal and transverse folds, and include domes, basins, culminations, and saddles.

(9) All of the folds described form at the same time as or just prior to faulting. For faults that intersect the Earth's surface, the associated folds develop syndepositionally. Synfolding sedimentary deposits are thicker in the hinges of synclines and thinner in the hinges of anticlines; water-depth–dependent facies are deeper in synclines than anticlines. Coarser grained facies tend to accumulate at anticlines (intrabasin highs) associated with fault segment boundaries and relay ramps.

REFERENCES CITED

Anders, M. H., and R. W. Schlische, 1994, Overlapping faults, intrabasin highs, and the growth of normal faults: Journal of Geology, v. 102, p. 165–180.

Bally, A. W., D. Bernoulli, G. A. Davis, and L. Montadert, 1981, Listric normal faults: Oceanological Acta, 26th International Geological Congress, Paris, p. 87–101.

Barnett, J. A. M., J. Mortimer, J. H. Rippon, J. J. Walsh, and J. Watterson, 1987, Displacement geometry in the volume containing a single normal fault: AAPG Bulletin, v. 71, p. 925–937.

Barrientos, S. E., R. S. Stein, and S. N. Ward, 1987, Comparison of the 1959 Hebgen Lake, Montana, and the 1983 Borah Peak, Idaho, earthquakes from geodetic observations: Seismological Society of America Bulletin, v. 77, p. 784–808.

Bradshaw, G. A., and M. D. Zoback, 1988, Listric normal faulting, stress refraction, and the state of stress in the Gulf Coast basin: Geology, v. 16, p. 271–274.
Chapman, G. R., S. J. Lippard, and J. E. Martyn, 1978, The stratigraphy and structure of the Kamasia Range, Kenya rift valley: Journal of the Geological Society (London), v. 135, p. 265–281.
Childs, C., J. Watterson, and J. J. Walsh, 1995, Fault overlap zones within developing normal fault systems: Journal of the Geological Society (London), v. 152, p. 535–550.
Cowie, P. A., and C. H. Scholz, 1992a, Displacement-length scaling relationship for faults: data synthesis and discussion: Journal of Structural Geology, v. 14, p. 1149–1156.
Cowie, P. A., and C. H. Scholz, 1992b, Physical explanation for displacement-length relationship of faults using a post-yield fracture mechanics model: Journal of Structural Geology, v. 14, p. 1133–1148.
Davis, G. A., and G. S. Lister, 1988, Detachment faulting in continental extension: perspectives from the southwestern U.S. Cordillera: Geological Society of America Special Paper 218, p. 133–159.
Davison, I., 1986, Listric normal fault profiles: calculation using bed-length balance and fault displacement: Journal of Structural Geology, v. 8, p. 209–210.
Davison, I., 1987, Normal fault geometry related to sediment compaction and burial: Journal of Structural Geology, v. 9, p. 393–401.
Davison, I., 1994, Linked faults systems; extensional, strike-slip and contractional, *in* P. L. Hancock, ed., Continental deformation: New York, Pergamon, p. 121–142.
Dawers, N. H., and M. H. Anders, 1995, Displacement-length scaling and fault linkage: Journal of Structural Geology, v. 17, p. 607–614.
Dawers, N. H., M. H. Anders, and C. H. Scholz, 1993, Growth of normal faults; displacement–length scaling: Geology, v. 21, p. 1107–1110.
de Matos, R. M. D., 1993, Geometry of the hanging wall above a system of listric normal faults—a numerical solution: AAPG Bulletin, v. 77, p. 1839–1859.
Dula, W. F., Jr., 1991, Geometric models of listric normal faults and rollover folds: AAPG Bulletin, v. 75, p. 1609–1625.
Elliott, D., 1976, Energy balance and deformation mechanisms of thrust sheets: Philosophical Transactions, Royal Society of London, v. A283, p. 289–312.
Fonseca, J., 1988, The Sou Hills: a barrier to faulting in the central Nevada seismic belt: Journal of Geophysical Research, v. 93, p. 475–489.
Gawthorpe, R. L., and J. M. Hurst, 1993, Transfer zones in extensional basins: their structural style and influence on drainage development and stratigraphy: Journal of the Geological Society (London), v. 150, p. 1137–1152.
Gibbs, A. D., 1983, Balanced cross-section construction from seismic sections in areas of extensional tectonics: Journal of Structural Geology, v. 5, p. 153–160.
Gibson, J. R., J. J. Walsh, and J. Watterson, 1989, Modelling of bed contours and cross-sections adjacent to planar normal faults: Journal of Structural Geology, v. 11, p. 317–328.
Gillespie, P. A., J. J. Walsh, and J. Watterson, 1992, Limitations of dimension and displacement data from single faults and the consequences for data analysis and interpretation: Journal of Structural Geology, v. 14, p. 1157–1172.
Groshong, R. H., Jr., 1989, Half-graben structures: balanced models of extensional fault-bend folds: Geological Society of America Bulletin, v. 101, p. 96–105.
Groshong, R. H., 1994, Area balance, depth to detachment, and strain in extension: Tectonics, v. 13, p. 1488–1497.
Hamblin, W. K., 1965, Origin of "reverse drag" on the downthrown sides of normal faults: Geological Society of America Bulletin, v. 76, p. 1145–1164.
Hancock, P. L., and A. A. Barka, 1987, Kinematic indicators on active normal faults in western Turkey: Journal of Structural Geology, v. 9, p. 573–584.
Harding, T. P., 1984, Graben hydrocarbon occurrences and structural style: AAPG Bulletin, v. 68, p. 333–362.
Hatcher, R. D., Jr., 1994, Structural geology: principles, concepts, problems: Englewood Cliffs, New Jersey, Prentice Hall, 525 p.
Jackson, J. A., 1987, Active normal faulting and crustal extension, *in* M. P. Coward, J. F. Dewey, and P. L. Hancock, eds., Continental extensional tectonics: Geological Society Special Publication 28, p. 3–17.
Jackson, J., and M. Leeder, 1994, Drainage systems and the development of normal faults: an example from Pleasant Valley, Nevada: Journal of Structural Geology, v. 16, p. 1041–1059.
Jackson, J., and D. McKenzie, 1983, The geometrical evolution of normal fault systems: Journal of Structural Geology, v. 5, p. 471–482.
Jackson, J. A., and N. J. White, 1989, Normal faulting in the upper continental crust: observations from regions of active extension: Journal of Structural Geology, v. 11, p. 15–36.
Kerr, H. G., N. White, and J.-P. Brun, 1993, An automatic method for determining three-dimensional normal fault geometries: Journal of Geophysical Research, v. 98, p. 17,837–17,857.
Larsen, P.-H., 1988, Relay structures in a Lower Permian basement-involved extension system, east Greenland: Journal of Structural Geology, v. 10, p. 3–8.
Laubscher, H. P., 1982, Die Südostecke des Rheingrabens—ein kinematisches und dynamisches problem: Eclogae Helvetiae, v. 75, p. 101–116.
Leeder, M. R., and R. L. Gawthorpe, 1987, Sedimentary models for extensional tilt-block/half-graben basins, *in* M. P. Coward, J. F. Dewey, and P. L. Hancock, eds., Continental extensional tectonics: Geological Society Special Publication 28, p. 139–152.
Linsley, P. N., H. C. Potter, G. McNab, and D. Racher, 1980, The Beatrice field, Inner Moray Firth, U.K. North Sea, *in* M. T. Halbouty, ed., Giant oil and gas fields of the decade 1968–1978: AAPG Memoir 30, p. 117–129.
Machette, M. N., S. F. Personius, A. R. Nelson, D. P. Schwartz, and W. R. Lund, 1991, The Wasatch fault zone, Utah—segmentation and history of Holocene earthquakes: Journal of Structural Geology, v. 13, p. 137–149.
Marrett, R., and R. W. Allmendinger, 1991, Estimates of strain due to brittle faulting: sampling of fault populations: Journal of Structural Geology, v. 13, p. 735–738.
Marrett, R., and R. W. Allmendinger, 1992, Amount of extension on "small" faults: an example from the Viking Graben: Geology, v. 20, p. 47–50.
Mitra, S., 1993, Geometry and kinematic evolution of inversion structures: AAPG Bulletin, v. 77, p. 1159–1191.
Morley, C. K., R. A. Nelson, T. L. Patton, and S. G. Munn, 1990, Transfer zones in the East African rift system and their relevance to hydrocarbon exploration in rifts: AAPG Bulletin, v. 74, p. 1234–1253.
Muraoka, H., and H. Kamata, 1983, Displacement distribution along minor fault traces: Journal of Structural Geology, v. 5, p. 483–495.
Murray, G. E., 1961, Geology of the Atlantic and Gulf coastal province of North America: New York, Harper Brothers, 692 p.
Olsen, P. E., D. V. Kent, B. Cornet, W. K. Witte, and R. W. Schlische, in press, High-resolution stratigraphy of the Newark rift basin (early Mesozoic, eastern North America): Geological Society of America Bulletin, v. 107.
Peacock, D. C. P., and D. J. Sanderson, 1991, Displacements, segment linkage and relay ramps in normal fault zones: Journal of Structural Geology, v. 13, p. 721–733.
Peacock, D. C. P., and X. Zhang, 1993, Field examples and numerical modelling of oversteps and bends along normal faults in cross-section: Tectonophysics, v. 234, p. 147–167.
Reynolds, D. J., 1994, Sedimentary basin evolution: tectonic and climatic interaction: Ph.D. thesis, Columbia University, New York, 331 p.
Roberts, A., and G. Yielding, 1994, Continental extensional tectonics, *in* P. L. Hancock, ed., Continental deformation: New York, Pergamon, p. 223–250.

Roberts, A. M., M. E. Badley, J. D. Price, and I. W. Huck, 1990, The structural history of a transtensional basin: Inner Moray Firth, NE Scotland: Journal of the Geological Society (London), v. 147, p. 87–103.

Roberts, A. M., J. D. Price, and T. S. Olsen, 1991, Late Jurassic half-graben control on the siting and structure of hydrocarbon accumulations: UK/Norwegian Central Graben, *in* R. F. P. Hardman and J. Brooks, eds., Tectonic events responsible for Britain's oil and gas reserves: Geological Society Special Publication 55, p. 229–257.

Robson, D. A., 1971, The structure of the Gulf of Suez (Clysmic) rift, with special reference to the eastern side: Journal of the Geological Society (London), v. 127, p. 247–276.

Rosendahl, B. R., 1987, Architecture of continental rifts with special reference to east Africa: Annual Review of Earth and Planetary Science, v. 15, p. 445–503.

Rowan, M. G., and R. Kligfield, 1989, Cross section restoration and balancing as aid to seismic interpretation in extensional terranes: AAPG Bulletin, v. 73, p. 955–966.

Schlische, R. W., 1991, Half-graben filling models: implications for the evolution of continental extensional basins: Basin Research, v. 3, p. 123–141.

Schlische, R. W., 1992, Structural and stratigraphic development of the Newark extensional basin, eastern North America: implications for the growth of the basin and its bounding structures: Geological Society of America Bulletin, v. 104, p. 1246–1263.

Schlische, R. W., 1993, Anatomy and evolution of the Triassic–Jurassic continental rift system, eastern North America: Tectonics, v. 12, p. 1026–1042.

Schlische, R. W., and M. H. Anders, in press, Stratigraphic effects and tectonic implications of the growth of normal faults and extensional basins, *in* K. K. Beratan, ed., Reconstructing the structural history of Basin and Range extension using sedimentology and stratigraphy: Geological Society of America Special Paper 303.

Schwartz, D. P., and K. J. Coppersmith, 1984, Fault behavior and characteristic earthquakes: examples from the Wasatch and San Andreas fault zones: Journal of Geophysical Research, v. 89, p. 5681–5698.

Shelton, J. W., 1984, Listric normal faults: an illustrated summary: AAPG Bulletin, v. 68, p. 801–815.

Stein, R. S., and S. E. Barrientos, 1985, Planar high-angle faulting in the Basin and Range: geodetic analysis of the 1983 Borah Peak, Idaho, earthquake: Journal of Geophysical Research, v. 90, p. 11,355–11,366.

Stein, R. S., G. C. P. King, and J. B. Rundle, 1988, The growth of geological structures by repeated earthquakes; 2. field examples of continental dip-slip faults: Journal of Geophysical Research, v. 93, p. 13,319–13,331.

Stewart, I. S., and P. L. Hancock, 1991, Scales of structural heterogeneity within neotectonic normal fault zones in the Aegean region: Journal of Structural Geology, v. 13, p. 191–204.

Trudgill, B., and J. Cartwright, 1994, Relay-ramp forms and normal fault linkages, Canyonlands National Park, Utah: Geological Society of America Bulletin, v. 106, p. 1143–1157.

Walsh, J. J., and J. Watterson, 1987, Distributions of cumulative displacement and seismic slip on a single normal fault surface: Journal of Structural Geology, v. 9, p. 1039–1046.

Walsh, J. J., and J. Watterson, 1988, Analysis of the relationship between displacements and dimensions of faults: Journal of Structural Geology, v. 10, p. 239–247.

Walsh, J. J., and J. Watterson, 1991, Geometric and kinematic coherence and scale effects in normal fault systems, *in* A. M. Roberts, G. Yielding, and B. Freeman, eds., The geometry of normal faults: Geological Society Special Publication 56, p. 193–203.

Walsh, J. J., and J. Watterson, 1992, Populations of faults and fault displacements and their effects on estimates of fault-related regional extension: Journal of Structural Geology, v. 14, p. 701–712.

Walsh, J. J., J. Watterson, and G. Yielding, 1991, The importance of small-scale faulting in regional extension: Nature, v. 351, p. 391–393.

Watterson, J., 1986, Fault dimensions, displacements and growth: Pure and Applied Geophysics, v. 124, p. 365–373.

Wheeler, G., 1939, Triassic fault-line deflections and associated warping: Journal of Geology, v. 47, p. 337–370.

White, N. J., and G. Yielding, 1991, Calculating normal fault geometries at depth: theory and examples, *in* A. M. Roberts, G. Yielding, and B. Freeman, eds., The geometry of normal faults: Geological Society Special Publication 56, p. 251–260.

White, N. J., J. A. Jackson, and D. P. McKenzie, 1986, The relationship between the geometry of normal faults and that of the sedimentary layers in their hanging walls: Journal of Structural Geology, v. 8, p. 897–909.

Withjack, M. O., and D. J. Drickman Pollock, 1984, Synthetic seismic-reflection profiles and rift-related structures: AAPG Bulletin, v. 68, p. 1160–1178.

Withjack, M. O., and E. T. Peterson, 1993, Prediction of normal-fault geometries—a sensitivity analysis: AAPG Bulletin, v. 77, p. 1860–1873.

Withjack, M. O., K. E. Meisling, and L. R. Russell, 1989, Forced folding and basement-detached normal faulting in the Haltenbanken area, offshore Norway, *in* A. J. Tankard and H. R. Balkwill, eds., Extensional tectonics and stratigraphy of the North Atlantic margins: AAPG Memoir 46, p. 567–575.

Withjack, M. O., J. Olson, and E. Peterson, 1990, Experimental models of extensional forced folds: AAPG Bulletin, v. 74, p. 1038–1054.

Xiao, H., and J. Suppe, 1992, Origin of rollover: AAPG Bulletin, v. 76, p. 509–529.

Young, S. S., R. W. Schlische, and R. V. Ackermann, 1995, Micro-normal fault populations in Mesozoic rift basins: length-displacement scaling relations (abs.): Geological Society of America Abstracts with Programs, v. 27, p. 94.

Zhang, P., D. B. Slemmons, and F. Mao, 1991, Geometric pattern, rupture termination and fault segmentation of the Dixie Valley–Pleasant Valley active normal fault system, Nevada, U.S.A.: Journal of Structural Geology, v. 13, p. 165–176.

Zhang, Y. K., 1994, Mechanics of extensional wedges and geometry of normal faults: Journal of Structural Geology, v. 16, p. 725–732.

ABOUT THE AUTHOR

Roy W. Schlische

Roy W. Schlische is an assistant professor of geology at Rutgers University. He received his B.A. degree from Rutgers and his M.A. degree and Ph.D. from Columbia University. His research interests include the structural and stratigraphic evolution of extensional basins, the geometry and causes of rift basin inversion, length-displacement scaling relations for normal faults, the mechanics of fault growth, analysis of fracture populations, and tectonic geomorphology.